DEVELOPMENT OF BREAST PHANTOMS FOR ULTRA-WIDEBAND (UWB) MICROWAVE IMAGING SYSTEMS

NUR SYUHADA BINTI AYOB

UNIVERSITI SAINS MALAYSIA

2023

DEVELOPMENT OF BREAST PHANTOMS FOR ULTRA-WIDEBAND (UWB) MICROWAVE IMAGING SYSTEMS

by

NUR SYUHADA BINTI AYOB

Thesis submitted in fulfilment of the requirements
for the degree of
Doctor of Philosophy

August 2023

ACKNOWLEDGEMENT

I would want to express my gratitude to Allah SWT, the Almighty, for giving me the strength and opportunity to fulfil this task. Second, I want to express my gratitude to my main supervisor and co-supervisor, Dr Ramzun Maizan Ramli and Dr Nor Zakiah Yahaya, who helped me complete this project. They supported me through tough times and gave me priceless advice. Their drive and assistance made a significant difference in the project's success. In addition, I want to thank all the lecturers and staff from Pusat Pengajian Sains Fizik (PPSF), Pusat Pengajian Pengajian Jarak Jauh (PPPJJ), and Pusat Pengajian Kejuruteraan Elektrik dan Elektronik (PPEE), USM, who assisted me in completing this research and provided the necessary equipment. I want to thank my parents, brothers, and sisters for their help as well. Without that assistance, I would not have been able to properly complete my work. Last but not least, I'd like to thank everyone for their encouragement and for motivating me to continue on this project.

TABLE OF CONTENTS

LIST OF TABLES

Page

LIST OF FIGURES

Page

LIST OF SYMBOLS

Hz	Hertz
MHz	Megahertz
GHz	Gigahertz
m	Meter
mm	Millimetre
cm	Centimetre
ε'	Dielectric constant
ε''	Loss factor
σ	Conductivity
ε_∞	Infinite permittivity
ε_s	Static permittivity
τ	Relaxation time
ω	Angular frequency
ε_o	Free space's permittivity
σ_s	Static conductivity
Γ	Reflection coefficient
Z	Impedance
Y	Admittance

LIST OF ABBREVIATIONS

UWB	Ultra-wideband
WHO	World Health Organization
GLOBOCAN	Global Cancer Observatory: CANCER TODAY
MRI	magnetic resonance imaging
CT	computed tomography
PVA-C	polyvinyl alcohol cryogel
DI	deionized water
FTC	freeze-thaw cycle
LA	lactic acid
PLA	polylactic acid
WLAN	wireless local area network
FCC	Federal Communication Commission
NN	neural network
PP	pattern recognition
TSAR	tissue sensing adaptive radar
DAS	delay and sum
EDS	enhanced delay and sum
ICNIRP	International Commission on Non-Ionizing Radiation Protection
PNA	Programmable Network Analyzer
VNA	Vector Network Analyzer
PTFE	Polytetrafluoroethylene
SMA	sub-miniature A
ISM	Industrial, Scientific and Medical band
FEM	finite element method
USM	Universiti Sains Malaysia

LIST OF APPENDICES

PEMBANGUNAN FANTOM PAYUDARA UNTUK SISTEM PENGIMEJAN GELOMBANG MIKRO JALUR-LEBAR ULTRA (UWB)

ABSTRAK

Pengimejan gelombang mikro ultra-lebar (UWB) adalah teknologi alternatif baru yang menjanjikan pengesanan tumor kanser payudara pada peringkat awal. Walau bagaimanapun, kit penentukuran diperlukan dalam kajian ini untuk mendapatkan keputusan yang tepat. Oleh itu, hantu payudara dengan sifat-sifat yang serupa dengan tisu payudara biologi (kulit, lemak, kelenjar, dan tumor) dicipta. 15 % polivinil alkohol (PVA), tepung gandum, dan air dinyahion digunakan untuk pembuatan fantom. Kepekatan tepung gandum, wf_c (%) yang berbeza (0 % hingga 50 %) telah ditambah kepada larutan PVA-C untuk menghasilkan pelbagai jenis tisu payudara. Asid laktik digunakan untuk tujuan pemeliharaan. Ciri-ciri dielektrik fantom yang direka diuji menggunakan sistem persediaan terdiri daripada penganalisis rangkaian vektor dan prob sepaksi dielektrik. Pekali pantulan diukur menggunakan sensor ekakutub tertebat rekaan. Julat frekuensi untuk semua ukuran antara 0.5 dan 50 GHz. Ciri-ciri dielektrik serupa dengan tisu payudara sebenar dalam fantom peniru kelenjar dan tumor yang direka. Ciri-ciri dielektrik phantom rekaan didapati mirip dengan tisu kelenjar dan tumor sebenar. Kepekatan tepung gandum, wf_c (%) sebanyak 79.33 %, 124.4 %, 44.13 % dan 25.56 % diperolehi menggunakan model ramalan I ditunjukkan boleh digunakan untuk mensimulasikan kulit, lemak, kelenjar dan tisu tumor, masing-masing. Hasilnya juga menunjukkan persetujuan dengan model Cole-Cole untuk fantom kulit, lemak, kelenjar, dan tumor. Kajian ini juga mendapati bahawa kepekatan tepung gandum, wf_c (%) dalam fantom payudara berasaskan PVA-C boleh ditentukan menggunakan sensor ekakutub tertebat.

DEVELOPMENT OF BREAST PHANTOMS FOR ULTRA-WIDEBAND (UWB) MICROWAVE IMAGING SYSTEMS

ABSTRACT

Ultra-wideband (UWB) microwave imaging is a promising new alternative technology for detecting breast cancer tumours in the early stages. However, the calibration kit is required in this study to obtain accurate results. Therefore, breast phantoms with properties similar to biological breast tissues (skin, fat, gland, and tumor) were created. 15 % polyvinyl alcohol (PVA), wheat flour, and deionized water were used for the fabrication of phantoms. Different wheat flour concentrations, wf_c (%) (0 % to 50 %) were added to the PVA-C solution to fabricate different types of breast tissues. Lactic acid was used for preservation purposes. The dielectric properties of the fabricated phantoms were tested utilising a setup system consisting of a vector network analyzer and a dielectric coaxial probe. The reflection coefficients were measured using a fabricated insulated monopole sensor. The frequency range for all measurements was between 0.5 and 50 GHz. The dielectric properties of the fabricated phantom were found to be similar to those of real gland and tumor tissues. The wf_c (%) of 79.33 %, 124.4 %, 44.13 % and 25.56 % acquired using the prediction model I have shown can be used to simulate skin, fat, gland, and tumor tissues, respectively. The results also showed agreement with the Cole-Cole model for skin, fat, gland, and tumor phantoms. This research also found that the wf_c (%) in PVA-C-based breast phantoms can be determined using an insulated monopole sensor.

CHAPTER 1

INTRODUCTION

1.1 Research Background

The potential advantages of microwave imaging for biological applications have been studied for more than 40 years, and several papers, books, and editorials have been published (Conceição et al., 2016; Fear & Ph, 2005; Iskander & Durney, 1980). Non-destructive testing and evaluation (NDT&E), the detection of concealed weapons at security checkpoints, structural health monitoring, and through-the-wall imaging are just a few of the applications of microwave imaging. Microwave frequencies range from 300 MHz to 300 GHz, with wavelengths ranging from 1 mm to 1 m. Microwave imaging studies for breast cancer detection have recently gained popularity. Microwave imaging heavily relies on the distinction between normal and malignant tissue dielectric properties.

According to World Health Organization (WHO) estimates, cancer is the first and second leading cause of death worldwide in 2019 (World Health Organization, 2020). Breast cancer is the most common cancer in women, having surpassed lung cancer as the malignancy with the most diagnoses. According to the International Agency for Research on Cancer's GLOBOCAN 2020 cancer incidence and mortality forecasts, there will be 2.3 million new cases (11.7 %) and 685,000 deaths worldwide in 2020 (Sung et al., 2021). Three million new cases and 1 million deaths are estimated for 2040. However, breast cancer’s survival rate has increased in the past decades because of early detection by screening (Berry et al., 2005; Rosa & Radünz, 2012; Saadatmand et al., 2015).

Mammography is the widely applied imaging method for breast cancer detection at an early stage. It used X-rays to detect the tumors in the breast. However, there are some negative aspects, such as uncomfortable breast compression and ionizing radiation exposure (Hellquist et al., 2015; Onega et al., 2016). Additionally, because younger women's breast tissues tend to be denser than those of older women (those under 40), it is less effective for them (Salem et al., 2013). Ultrasound is an excellent alternative method as it can detect tiny breast cancer tissue in young women not seen in mammography (Ozmen et al., 2015). It has a limitation as a screening tool because of the false-negative rate (Rankin, 2000). MRI is more expensive and time-consuming, yet it offers the highest sensitivity to breast cancer (Bansal et al., 2013; Hassan & El-Shenawee, 2011; Roganovic et al., 2015). The disadvantages of current screening methods have led many researchers to find a solution by exploring a new imaging technique.

Microwave imaging for breast cancer detection has several advantages over other methods. The most crucial finding is that the electrical properties, permittivity, and conductivity of malignant breast tumor tissues are significantly different from those of normal surrounding breast tissues. The projected variance was five to ten times greater (Fear et al., 2002). Perhaps the most advantageous aspect of this technology is the ability to image the breast without the use of ionizing radiation, which enables safe and frequent examinations of all women, regardless of age or condition (e.g., in pregnancy). It also offers patients a non-invasive imaging technique for breast cancer screening in which patients simply lay face down on an exam table with their breasts inserted into the device through an opening in the bed (Janjic et al., 2022). Microwave imaging systems have the potential to be low-cost and portable for

use in early breast cancer detection, as well as taking less time to conduct (Islam et al., 2019; Vasquez et al., 2016).

To detect breast cancer, three different approaches have been researched. There are three types of methods: passive, hybrid, and active, as seen in Figure 1.1. (Aldhaeebi et al., 2020; Khalil et al., 2012). A passive approach involves using a radiometry device to measure the temperature differential between healthy and malignant breast tissue (Mouty et al., 2000). Thermal acoustic detection uses microwave sensors and ultrasonic transducers combined in a hybrid approach (Cui et al., 2017). Microwave signals are used in active methods to illuminate breast tissues. Within a specific microwave frequency range, the difference in dielectric properties between malignant and normal breast tissues is measured.

The main approaches in the active method are tomography and radar-based. Tomography is typically an iterative process and represents a nonlinear inverse problem that requires significant computational resources to provide dielectric properties. In contrast, radar-based approaches employ an external microwave source to illuminate breast tissues with ultra-wideband (UWB) signals (Bindu et al., 2006b). Unlike microwave tomography, radar-based microwave imaging focuses on the tumor rather than the entire breast. As a result, signal processing is simpler than in microwave tomography. Radar-based microwave imaging employs an ultra-wideband (UWB) pulse with frequencies ranging from low to high. The low-frequency band ensures adequate penetration depth, while the high-frequency band ensures adequate image resolution. As a result, low- and high-frequency bands can detect both deeply buried and very small tumors (Torrealba-Meléndez et al., 2014; Wenyi et al., 2005). This work will focus on radar-based microwave imaging.

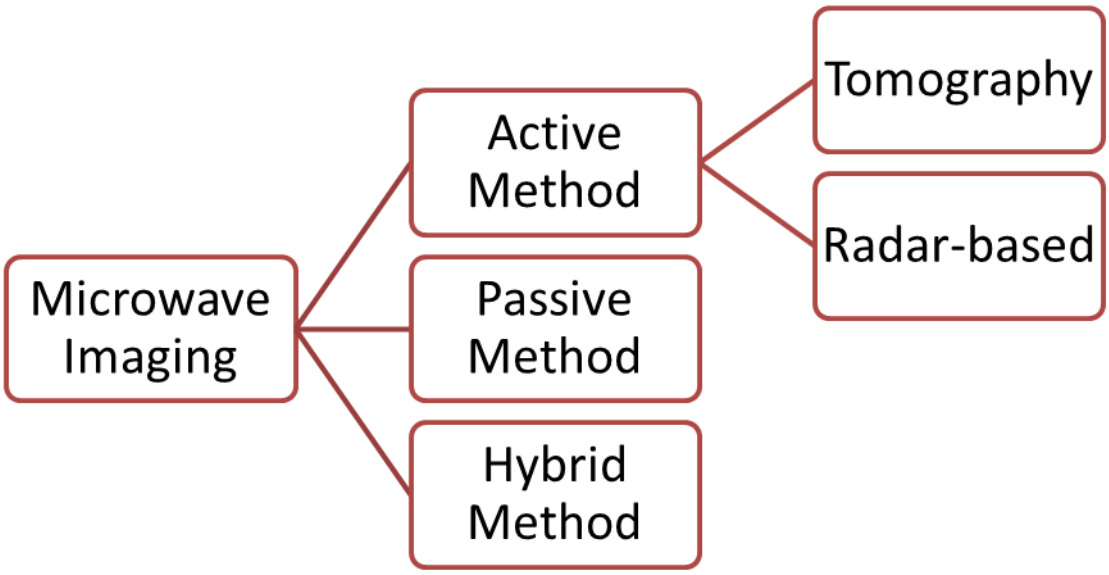

Figure 1.1 Type of microwave imaging

1.2 Problem Statements

Microwave imaging has yet to be commercialised for breast imaging since the study is still in its clinical phase (Janjic et al., 2021; Moloney et al., 2022). To evaluate the sensitivity and accuracy of breast tumor detection using microwave imaging, a comprehensive, quantitative experiment is required. The real human body must therefore be used to take precise and realistic measurements. The disadvantage is that human subjects will be subjected to the systems' or technologies' inherent dangers. It raises severe ethical questions because it involves safety risks. Therefore, the use of artificial breast tissue-mimicking phantoms will be the solution to this issue. The phantoms must possess properties of dielectric that are comparable in comparison to real breast tissues.

For microwave breast imaging, a variety of tissue-mimicking phantoms have been proposed in earlier investigations employing materials like gelatin (Croteau et al., 2009; Lai et al., 2010b; Porter et al., 2010), agar (Abu Bakar et al., 2011; Ostadrahimi et al., 2009), petroleum jelly (Alshehri, et al., 2011a; Alshehri et al., 2011;

AlShehri et al., 2011), TX151 (Klemm et al., 2009; Klemm et al., 2009a), Triton X-100 (Joachimowicz et al., 2016; Joachimowicz et al., 2014), and rubber (Garrett & Fear, 2015; Santorelli et al., 2015). But, the limitations are some phantoms contained toxic ingredients such as formaldehyde (Abu Bakar et al., 2011; Mashal et al., 2011), early studies proposed liquid-based phantoms which pose a significant barrier to the development of realistic, heterogeneous multilayer phantoms that resemble breasts (Croteau et al., 2009; Lai et al., 2010b; Porter et al., 2010) and for dielectric measurements, the majority of the proposed phantoms only work up to 20 GHz (Croteau et al., 2009; Garrett & Fear, 2015). There are also not many studies that suggested prediction methods for the purposeful fabrication of phantoms with specified electromagnetic properties (Castello-Palacios et al., 2017; La Gioia et al., 2018). Consequently, it is essential to develop a breast phantom that can be used over a wide frequency range (> 20 GHz) for dielectric characterisation, contains harmless components, and uses material that maintained its structural stability.

1.3 Research Questions

The research questions for this study are as follows:

i. What are the effects of various wheat flour concentrations, wf_c (%) on the dielectric properties and conductivity of PVA-C-based phantoms?
ii. What are the optimum wheat flour concentrations, wf_c (%) for breast phantom developments?
iii. What are the Cole-Cole parameters for breast phantoms developments?
iv. What are the insulated monopole sensor's reflection coefficient values obtained from experimental data, the prediction method, and the finite element method (FEM)?

1.4 Research Objectives

The research's primary goal is to develop physically homogeneous breast (skin, fat, gland and tumor) tissue-mimicking phantoms with dielectric properties similar to real breast tissues (skin, fat, gland and tumor). The sub-objectives in this work are:

i. To investigate the effects of various wheat flour concentrations, wf_c (%) on the dielectric properties and conductivity of PVA-C-based phantoms.

ii. To create prediction breast phantom models that can predict the optimum wheat flour concentration, wf_c (%) for breast phantom developments using MATLAB software.

iii. To establish the experimental data-based Cole-Cole parameters for breast phantom developments using MATLAB software.

iv. To compare the insulated monopole sensor's reflection coefficient values obtained from experimental data, the prediction method using MATLAB software, and the finite element method (FEM) using COMSOL Multiphysics software.

1.5 Significance of Study

The research's significance is in the production of novel prediction models and methods to develop breast phantoms that accurately mimic real breast tissue (skin, fat, gland, tumor) for microwave breast imaging at frequencies up to 50 GHz.

1.6 Scope of study

Using wheat flour as the material that will modify the dielectric properties and polyvinyl alcohol (PVA) cryogel as the gelling agent, this study will develop breast phantoms that can mimic the real human breast in terms of dielectric properties.

Different wheat flour concentrations, wf_c (%) will be used to fabricate the phantoms The UWB frequency range, 0.5 to 50 GHz, will be used for data measurements.

1.7 Research Process

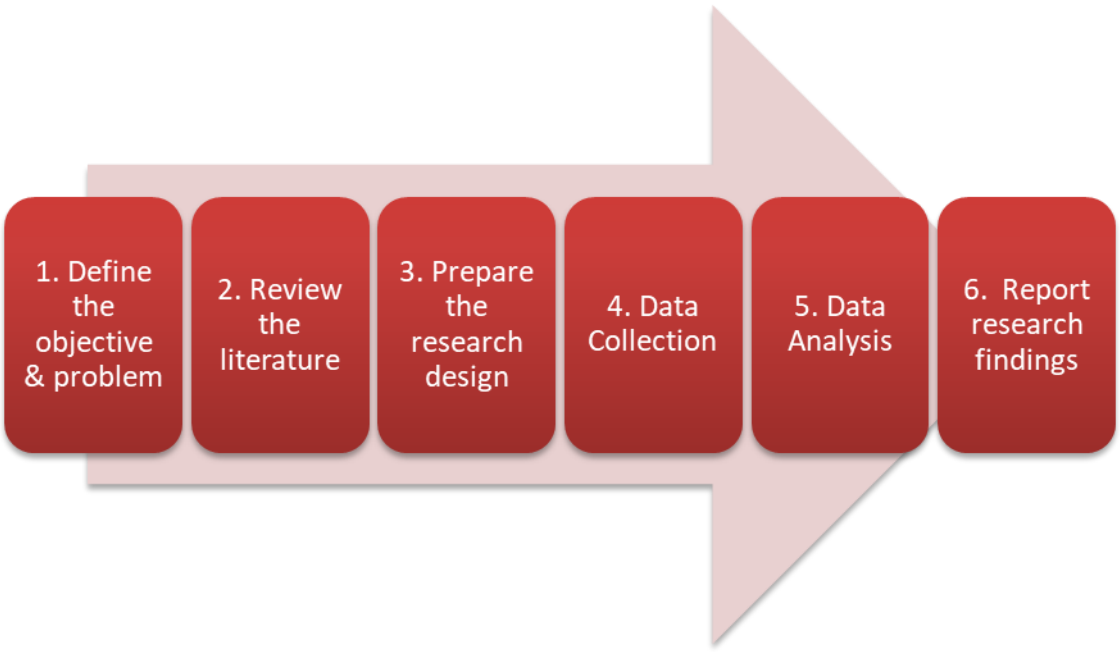

Figure 1.2 The steps for the research processes

1.8 Thesis Outline

Five central chapters will include in this thesis. Chapter one is the introduction. It will discuss the background of the main elements in this study, the problem statements regarding this study, its objectives, and its scope. Chapter two is the literature review. This chapter will briefly discuss the studies done by other researchers regarding the same matter in this work. It will also discuss the main concepts in this work's essential areas. Chapter three is the chapter that will cover the materials used and the methodology of this work. Chapter four will cover the overall results of this study and discuss the results obtained. The last chapter will be in chapter five. It will be the chapters that will conclude the comprehensive research and cover the limitations that occur during the study and suggestions for future works.

CHAPTER 2

LITERATURE REVIEW

2.1 Human Breast Anatomy

Breast anatomy falls under the category of complicated surface anatomy in humans. Adult female breasts typically have a projecting cone shape with a circular base that measures 7-8 cm in diameter. It is comprised of glandular, connective, and adipose tissue. Mammary glands are modified sweat glands found in glandular tissues. They have between 15 and 20 lactiferous ducts that converge and connect to the nipple. An areola, a circle of pigmented skin around the nipple, is present. The areola typically has a diameter of 2.5 cm. Each duct has 20 to 40 lobes, which are further split into acini. Acini, which are small glands, are in charge of generating milk in response to usual hormonal fluctuations. By expanding across the breast and filling in the spaces between the lobes, adipose (fatty) tissues give the breast its shape and size. To support the breast, fibrous or connective tissue known as Cooper's ligament grows around the lobes and lobules. Last but not least, a flexible connective tissue called retro-mammary fat separates the breast from the main pectoralis muscle.

Beginning with birth, puberty, pregnancy, breastfeeding, and finishing with menopause, the breast experiences the biggest changes. Breast cancer has primarily affected older women, 50 years and older. However, breast cancer also affects younger people due to lifestyle choices and other circumstances. In the United States, women under the age of 45 account for around 10.2 % - 11 % of all new instances of breast cancer (Centers for Disease Control and Prevention, 2020; National Cancer Institute, 2020). Breast cancer develops when the breast cells start to proliferate unchecked. A tumor is produced by abnormally expanding cells, and it can be identified and seen on an X-ray or felt as a bump by self-examination (American Cancer Society, 2021). In

younger women, the breast mostly consists of thick glandular tissue with a modest amount of adipose (fatty) tissue. Consequently, breast composition is typically firmer and denser in younger women (Checka et al., 2012). While the loss of oestrogen hormones causes a major shift in breast tissue consistency in older women, particularly during menopause. Fat takes the place of the glandular tissue's lobes, making the breast less dense and firm overall. The breast parenchyma's lobular units' terminal ends are where the majority of tumors grow. Because there is more glandular tissue in the super-external region of the breast, half of the tumors are found here (Cirolla, 2013; Gabriel et al., 2016; O'Halloran et al., 2016). The formation of the female breast is shown in Figure 2.1 and Figure 2.2.

Breast cancer is classified as in situ (non-invasive) or invasive (invasive). Breast cancer that remains within the ducts and basement membrane of the lobules is known as in-situ or non-invasive breast cancer. The cancer cells will spread into the neighbouring healthy tissues past the duct and lobule basement membranes. The most common types of invasive breast cancer are invasive ductal carcinoma (IDC) and invasive lobular carcinoma (ILC), while ductal carcinoma in situ (DCIS) and lobular carcinoma in situ (LCIS) are the most common types of non-invasive breast cancer (LCIS). In contrast to ILC, which accounts for 10% of cases, IDC is the more common variant, accounting for 70% to 80% of cases. Although LCIS enhances the likelihood of the cells turning into cancer cells, DCIS and LCIS are not the same forms of cancer (Sainsbury et al., 2000). A tumor's cell growth determines whether it is benign or malignant. Due to their rapid pace of replication, malignant tumours typically spread to other body parts and ravage the nearby healthy tissues. While cell development is restricted in benign tumours. If the cell compresses surrounding organs or releases

undesirable hormones, the benign tumor may become a cause for concern (O'Halloran et al., 2016).

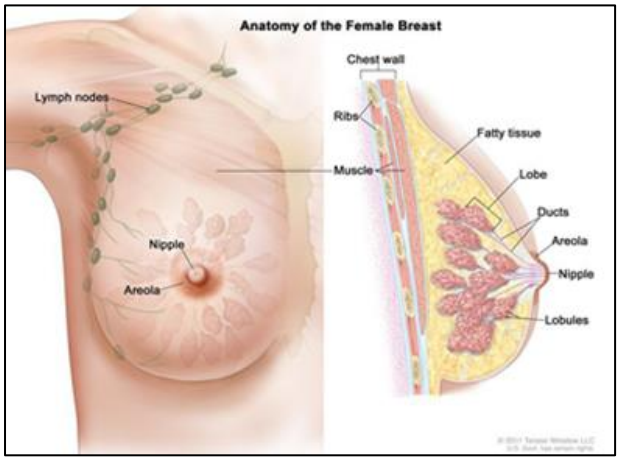

Figure 2.1 Anatomy of the breast. Front view (left) and side view (right). Image adapted from (National Breast Cancer Foundation, 2013)

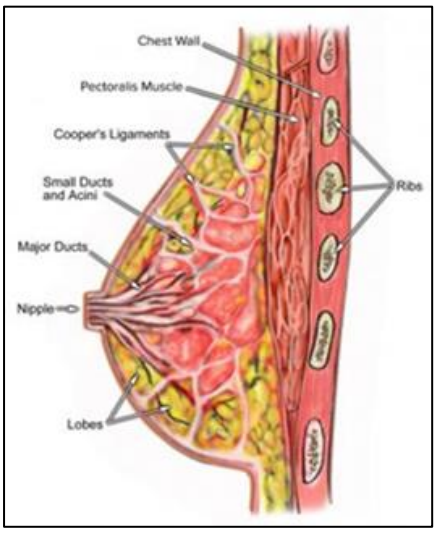

Figure 2.2 Breast anatomy shows its tissues (Gabriel et al., 2016)

2.2 Ultra-wideband (UWB) Microwave Breast Imaging

The ultra-wideband (UWB) has numerous applications in high-speed communications, including radars, short-range devices such as PC peripherals, and wireless local area and network communications (WLANs). Since 2002, the Federal

Communications Commission (FCC) has permitted imaging-related commercial use of 7.5 GHz UWB bands (3.1 to 10.6 GHz) (Federal Communications Commission, 2002).

As an alternative to traditional and existing modalities, UWB microwave imaging is a novel method for screening breast cancer. With UWB microwave imaging, the shortcomings of current technologies such as false signals, scans of low resolution, high costs, and patient distress are all can be resolved. Because of its high positive rate, affordable price, comfort, high data rate, minimal complexity, mobility, and low spectral power density, it is advantageous (Hassan & El-Shenawee, 2011). The fundamental is to penetrate breast tissue with UWB microwave signals and the backscattered signals will be analyzed which reveal the variations in dielectric properties of the tissues. As undesired tumor inside the breast has greater dielectric constants than healthy breast tissues, the back-scattered signal exhibits noteworthy fluctuations that might be exploited to detect them (Davis et al., 2008). Recent clinical studies have shown tremendous interest in microwave imaging, which has a detection accuracy of 80–90 % for tumors as small as 5–10 mm (Meaney et al., 2000). To detect breast cancer, researchers have recommended employing UWB microwave imaging (Alshehri & Khatun, 2009; Amdaouch et al., 2019; Kahar et al., 2015).

2.3 Relationship between Electromagnetic Waves and Biological Tissues

The core idea behind microwave imaging is how the electromagnetic field interacts with the human body. It depends on the tissue's value for the dielectric properties. When communicating with tissue in various amounts, electromagnetic waves can be emitted, absorbed, and reflected. Tumors can be detected at microwave frequencies due to the critical dielectric difference between normal and tumor tissues.

When interaction occurs, biological tissues can have multiple dielectric polarization effects or dispersion that contribute to their total permittivity. In particular, polarization occurs at specific frequencies and contributes to tissues' dielectric behavior (Foster & Schwan, 1989; Schwan & Foster, 1980). Figure 2.3 shows the polarization effects that occurred at different frequencies. The frequency band between infrared (10^{11} - 10^{14} Hz) and ultraviolet (10^{14} - 10^{17} Hz) has a dielectric dispersion caused by atomic and electronic polarizations. Both polarizations remain constant at microwave frequencies (10^{6} - 10^{9} Hz). The orientation (dipolar) is the primary dispersion mechanism in biological tissues at microwave frequencies. Water molecules in biological tissues have permanent dipole moments. A change in the real and imaginary parts of the relative permittivity will result from the rotation of the dipoles. The dispersion steps are known as γ-dispersion and δ-dispersion. The δ-dispersion is a weaker effect due to protein-bound water in biological tissues. Ionic conductivity is due to ions' free movements in biological tissues. Interfacial or space charge is correlated to charge accumulation at the tissue cell membrane. α-dispersion occurs at low frequencies ranging from Hz to kHz, whereas β-dispersion occurs at higher frequencies ranging from kHz to MHz (Figure 2.4).

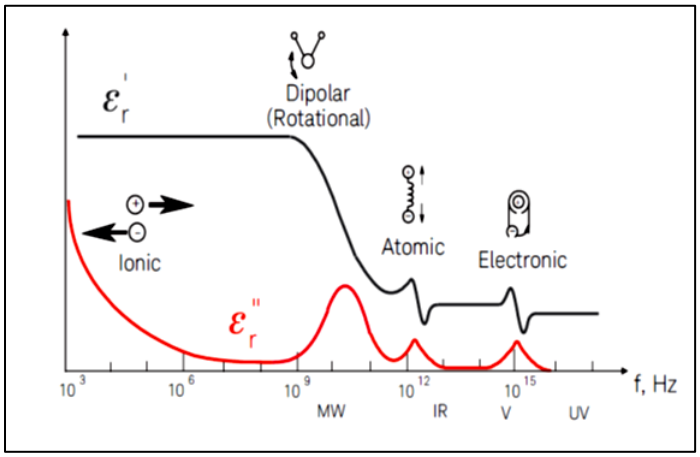

Figure 2.3 Frequency responses of different dielectric polarization effects (Keysight Technologies, 2020)

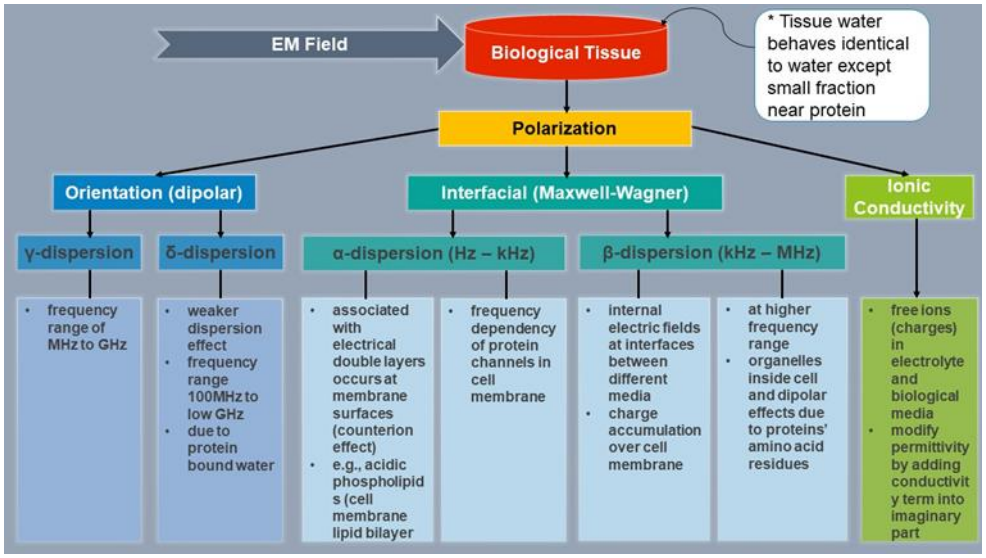

Figure 2.4 Interaction of the electromagnetic field and biological tissues (Li et al., 2016; Vorst et al., 2006)

All of the polarization mechanisms work together to gradually reduce the tissue's relative permittivity and dielectric losses as the frequency rises. Each polarization is described by dispersion steps. A relaxation time, τ characterizes each dispersion. Consequently, the complex relative permittivity, ε* is how biological tissues' permittivity is characterized. Relative permittivity is highly dependent on frequency (Gabriel et al., 1996; Schwan & Foster, 1980). The complex relative permittivity involving both the real and imaginary parts is written as

$$\varepsilon^* = \varepsilon' - j\varepsilon'' \tag{2.1}$$

The ability of biological tissues to keep in reserve energy when interacting with an external electric field is referred to as the real part of complex permittivity, ε'. Other names for it include “dielectric constant” and “relative permittivity”. The imaginary part of the permittivity, ε" also known as the “dielectric loss factor”, affects the tissues’ ability to absorb or attenuate energy.

The imaginary part of the complex permittivity is related to the conductivity, σ of biological tissues by the relationship, which is written as

$$\varepsilon'' = \frac{\sigma}{\varepsilon_0 \omega} \tag{2.2}$$

$$\sigma = \omega \varepsilon'' \varepsilon_0 \tag{2.3}$$

ε_0 is defined as the free space's permittivity, while ω is the electric field's angular frequency. The frequency-inverse decay of σ's contribution to the total loss factor.

The proportion of the complex permittivity's imaginary to real parts. is known as the loss tangent or tan δ.

$$tan\,\delta = \frac{\varepsilon''}{\varepsilon'} = \frac{\sigma}{\omega \varepsilon' \varepsilon_0} \tag{2.4}$$

The loss tangent, tan δ, is also known as the dissipation factor, tangent loss, or tan delta (Keysight Technologies, 2020). The Kramers-Kronig relations link the real and imaginary parts of permittivity together so that they can't differ from one another independently (Foster & Schwan, 1989).

2.4 Dielectric Properties of Real Breast Tissues.

When the electromagnetic field interacts with the human body, the skin is the outermost and first area that is exposed to it. The skin will absorb some of the energy after an encounter. In a preliminary investigation, the dielectric characteristics of human skin at wavelengths between 1 and 10 cm were determined (England, 1950; England & Sharples, 1949). Since human blood vessels operate best at a temperature of 37 °C, that

temperature was used for the measurement. In a different investigation, the coaxial line method was used at frequencies equivalent to free space wavelengths between 6 and 17 cm, and a single-term Debye function was presented (Cook, 1951). The relative permittivity and conductivity of skin show good agreement with (England, 1950).

Experimental studies have been conducted for a frequency range of 10 Hz to 20 GHz using the Cole-Cole model by (Gabriel et al., 1996a). The study showed better results than those by (Cook, 1951; England, 1950; England & Sharples, 1949). The first measured permittivity data was presented for human skin in the millimeter-wave band over the band 60 to 100 GHz using a quasi-optical method. Permittivity models as frequency functions, such as Debye and Cole-Cole type equations, have been extrapolated. The results showed a better and broader range of dielectric properties for human skin than previous studies (Alabaster, 2003). Figure 2.5 showed a list of the frequency values used to calculate the skin's dielectric properties.

Investigations into the dielectric properties of various sorts of breast tissue are conducted in the 10 Hz to 50 GHz frequency range, similar to the skin (Campbell & Land, 1992; Chaudhary et al., 1984; Gabriel et al., 1996a). Then, ranging from 3 MHz to 3 GHz at 25° C, the dielectric properties of ex vivo normal and tumor breast tissues are investigated (Chaudhary et al., 1984). Normal and malignant breast tissues have significantly different dielectric properties, with the greatest permittivity variation occurring at frequencies less than 100 MHz. Furthermore, in the 20 kHz to 100 MHz frequency range, the dielectric properties of invasive tumors and the surrounding tissues were reported (Surowiec et al., 1988). There are three types of breast carcinoma identified. After that, the complex permittivity of four types of female breast tissue (adipose, glandular, benign, and malignant) at 3.2 GHz using in vivo methods are

measured (Campbell & Land, 1992). They asserted that the fact that (Surowiec et al., 1988) collected and stored their measurements in saline may have caused them to be inaccurate. In contrast to the breast tissue sample, the microwave frequencies might be more oriented toward saline. The results, however, demonstrated that while benign and malignant tumors have equivalent dielectric properties, the methods used could not tell them apart.

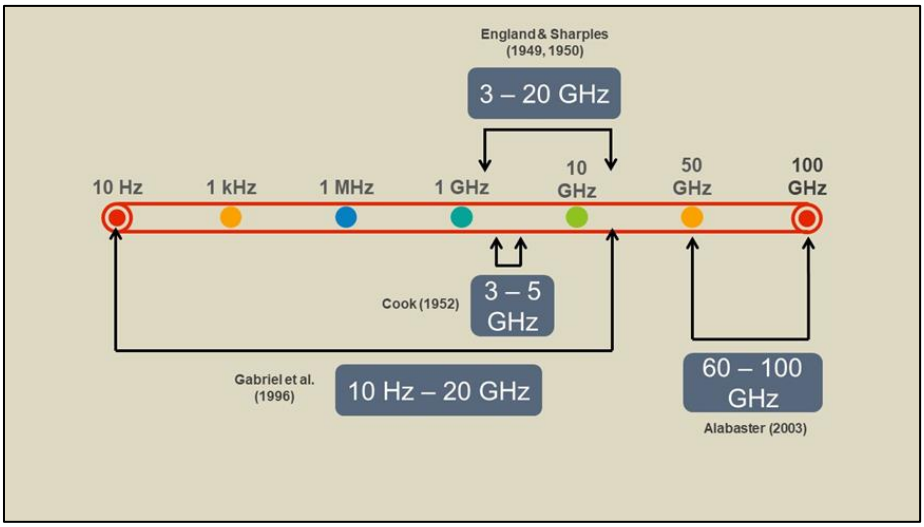

Figure 2.5 The frequency values used in previous studies to determine the dielectric properties of the skin (Alabaster, 2003; Cook, 1951; England, 1950; England & Sharples, 1949)

Between 50 and 900 MHz, a study was done on the dielectric properties of normal and tumor breast tissue (Joines et al., 1994). The mammary gland exhibits the most pronounced dielectric contrast, with average relative permittivity and conductivity differences of 6.4:1 and 3.8:1, respectively, which are generally consistent with the observations by (Chaudhary et al., 1984). Later, a team of researchers reviewed an experimental investigation for the 10 Hz to 20 GHz frequency range on the dielectric properties of breast fatty tissues. Additionally, they created a parametric model to explain in what way tissues' variants in their dielectric properties change with frequency (Gabriel et al., 1996; Gabriel et al., 1996b, 1996a).

A comparison between the experimental data and corresponding data from (Campbell & Land, 1992) and (Joines et al., 1994) showed a good agreement. Using a tomographic microwave imaging device clinical prototype, the dielectric properties of normal breast tissue are then estimated in vivo (Meaney et al., 2000). Normal tissue's permittivity values at 900 MHz on average are considerably higher than those that were previously depicted in the ex vivo experiments (Chaudhary et al., 1984; Joines et al., 1994). According to the study, there may be a link between the mean permittivity values and the radiographic density of the tissue. Between 0.5 and 30 GHz, the dielectric properties of breast cancer tissue metastasized lymph nodes, and healthy lymph nodes were all studied by (Choi et al., 2004). Bindu et al. (2006a) measured the dielectric contrast of breast tissues at 2.983 GHz using a confocal microwave method. Using a matching coupling medium (corn syrup), in vitro tests were performed on malignant inclusions in healthy breast tissue.

Research has been done on the normal breast tissue's dielectric properties derived after reduction procedures (Lazebnik et al., 2007). The proportion of adipose, glandular, and fibro-glandular tissue present in each sample used was categorized. The tissue was divided into three groups: Group 1 (0–30 % adipose tissue), Group 2 (31–84 % adipose tissue), and Group 3 (85–100 % adipose tissue). The group with more adipose tissue will have less desirable dielectric characteristics. The group with a larger fibro-glandular component will have higher values for conductivity and permittivity in difference. Additionally, normal breast tissue exhibits significant variability (Martellosio et al., 2017). Lazebnik et al. (2007) expanded their research to include the healthy, benign, and malignant breast tissues' dielectric properties collected during cancer procedures. In both studies, a very thorough database of dielectric properties for creating numerical breast phantom models was generated in addition to other useful

results on the division of tissues spanning a frequency range of 0.5 to 20 GHz. The measured dielectric values for malignant tissue agreed well with earlier investigations by (Chaudhary et al., 1984; Joines et al., 1994; Surowiec et al., 1988). In terms of statistics, the glandular tissues in the breast that are healthy and those that are malignant are identical. It is consistent with their findings that normal tissues' dielectric properties range widely, from extremely low, fat dielectric values to high, saline-like dielectric properties.

On the other hand, malignant tissues have high dielectric properties with a narrow range. Benign tissues have dielectric properties similar to normal breast tissues with decreased fat content. A rectangular resonant cavity perturbation approach was employed to assess the complex permittivity of breast tissues at the ISM band utilizing in vitro methods (Bindu & Mathew, 2008). Normal, malignant, and benign breast tissues were distinguished from one another based on dielectric properties and water content. According to the variance in the dielectric properties compared to the typical dielectric properties of breast tissue, benign and malignant breast cancers are distinguished. The difference in permittivity between malignant and healthy breast tissues is more than the difference between benign and healthy breast tissues.

The first experiment performed above 20 GHz was performed by Martellosio et al. (2017), who thoroughly examined the dielectric characteristics of breast tissues for the 0.5 to 50 GHz frequency range. More than 220 samples of tissue from a population of more than 50 people were obtained after surgery (ex vivo), and these samples were used for the measurements. Based on experimental findings, Cole-Cole models were developed for normal and tumor tissues and compared with (Lazebnik et al., 2007; Lazebnik et al., 2007). The outcomes, which the pathological study supported, showed

that the dielectric properties of normal tissues have greater variation than those of tumorous tissues. This difference is caused by differences in the adipose content of different tissues within the healthy breast. Despite this variance, the complex permittivity of tumor tissues is much greater than normal breast tissues in both the real and imaginary parts. This offers an adequate contrast up to 50 GHz to enable future millimetre-wave applications, including tissue identification during or after surgery and breast imaging. The recommendations of the International Commission on Non-Ionizing Radiation Protection (ICNIRP) addressed a millimetre-wave imaging compliance system for breast cancer detection as well as the distinction between normal and tumor tissues, a crucial parameter for several biomedical applications (Ziegelberger et al., 2020).

After that, a thorough investigation was done to study the properties of newly excised breast tissues obtained from cancer procedures that are normal, benign, or malignant (Cheng & Fu, 2018). Histology was used to determine whether the samples of recently resected breast tissues contained a benign, normal, or malignant tumor. Between 0.5 and 8 GHz, the microwave's effective conductivity and effective dielectric permittivity were measured. Breast cancer tissues had significantly higher effective relative permittivity and effective conductivity than benign tumors and much more than healthy breast tissue at each frequency. In both healthy and cancerous breast tissues, at 2.5 GHz, the standard deviation of each parameter was the smallest.

2.5 Breast Phantom for Microwave Breast Imaging

A "phantom" is a simulation tool that emulates the properties of human or animal tissue (Pogue & Patterson, 2006). Phantoms that closely resemble the physical qualities of the many types of tissues in the human body have been investigated and

built for testing a variety of medical imaging technology, such as ultrasound, magnetic resonance imaging (MRI), and computed tomography (CT).

After a few decades, mobile devices are now pervasive and integral to almost all of our daily activities. Due to the emission of electromagnetic energy by mobile phones and the growth of electromagnetic energy applications in diagnostic medical imaging, there is increased interest in a study on the interactions between electromagnetic energy and human biological tissues at microwave frequencies. Therefore, there is a much greater requirement for physical phantoms that can imitate the electromagnetic characteristics of tissues at these high frequencies. Previous studies have proposed many types of tissue-mimicking phantom for microwave breast imaging (Table 2.1). Materials with gelling agents, such as oil and saline, have generally been employed in phantom developments for microwave imaging to modify the dielectric properties (Guy, 1971; Ianniello et al., 2018). One of the earliest studies on breast phantom development was done for ultrasound imaging using oil-in-gelatin (Madsen et al., 2003; Madsen et al., 1982).

2.5.1 Oil-in-gelatin (Safflower Oil)

The first proposed is the project to develop tissue-like materials made from oil-in-gelatin that mimic the dielectric characteristics of numerous biological tissues in the human body (Lazebnik et al., 2005). For fat tissues and dry and wet skin, oil-in-gelatin dispersions were studied at microwave frequencies ranging from 0.5 to 20 GHz. Different volume percentages of a 50/50 solution of kerosene and safflower oil make up the gelatin-based components. The BSID algorithm is used to determine where a patient's breast surface is located from scattered UWB microwave signals (Winters et al., 2008). One of the simulators is a physically accurate phantom, which is used to evaluate how well the algorithm performs. The 3-D experimental breast phantom

comprises two different tissue-mimicking materials (Lazebnik et al., 2005) to simulate skin and fat. To test and enhance the tissue sensing adaptive radar (TSAR) scanning system between the frequencies of 50 MHz and 13.51 GHz, a few breast phantoms were made utilizing oil-in-gelatin materials (Croteau et al., 2009) (Figure 2.6 (a)). The amount of surfactant for the fat material increased for easier mixing and a more uniform fat material setting. Then, to model the dielectric properties of the breast over the 0.5 GHz to 13.5 GHz microwave frequency range, a realistic breast phantom is created by (Lai et al., 2010a, 2011). The oil-in-gelatin-based materials used same as those proposed by (Lazebnik et al., 2005). By combining ingredients comprised of various amounts of manufactured oil, homogeneous and heterogeneous phantoms are presented. Higher oil content materials don't exhibit any noticeable irregularities and can be used to create uniform breast phantoms with substantial adipose tissue. In comparison to previously published breast phantoms, dielectric measurement findings demonstrated that the phantoms could more accurately replicate the dielectric characteristics and variability of a human breast (Lazebnik et al., 2005).

The oil-in-gelatin mixture was then used to determine the chemical concentrations that produce phantoms with dielectric properties similar to fat (adipose tissue), skin, glands, and tumors (Porter et al., 2010). The breast phantom has a realistic radius of 6.5 cm and is made up of a skin layer 2 mm thick, various-sized adipose tissues, glands, and malignancies. A time-domain microwave method of detecting breast cancer was created by (Porter et al., 2010). The system's ability to identify tumors of various sizes and locations was tested using a phantom with a 2.5-mm thick skin layer filled with fat tissue components. Two separate-sized cylindrical tumors, each measuring 3 cm high and 2 cm or 1 cm in diameter, were evaluated (Porter et al., 2011). After that, Porter et al. (2011) tested the effectiveness of the same microwave imaging

technique using glandular phantoms (Figure 2.6 (b)). The measurements also included the healthy tissues of skin, fat, and gland, as well as a malignant tumor. More specifically, the measures presented here explore how the presence of various amounts of glandular material within the breast affects the ability to detect the tumor response. Later, Porter et al. (2012, 2013) provided a sophisticated testing scenario for the microwave time-domain breast cancer detection system employing phantoms of breasts with variable shapes. The analysis conducted by the study utilized the same tissue concentrations, mixing techniques, and electrical characteristics (Klemm et al., 2009). Three complete breast phantoms are created for each phantom using three distinct tumor sizes (0.5 cm, 1 cm, and 2 cm) and various oil volume percentages. The findings did not agree well with measurements made earlier on breast phantoms that were hemispherical (Porter et al., 2011). Studies show that uneven breast and skin shape are crucial elements that significantly affect the signals that are produced.

Mashal et al. (2011) presented a technique for creating anthropomorphic breast phantoms that are stable, heterogeneous, and have accurate dielectric characteristics (Figure 2.6 (c)). The phantoms were made from materials used by (Lazebnik et al., 2005). A nonidentical volumetric breast density classification is represented by each of the four realistic breast phantoms. The materials are stable for nine weeks if not in contact with air for extended periods, and the phantoms are rather strong and not readily harmed during mild handling. The materials are also resistant to oil (a 1:1 mixture of kerosene and safflower oil), which is a crucial quality for investigations where the phantoms must be submerged in a coupling solution. Later, inexpensive, non-toxic, and simple-to-manufacture phantoms were created, and their dielectric properties were first time evaluated in the frequency range of 0.5-50 GHz (Di Meo et al., 2019) (Figure 2.6 (d)).

(a) (b)

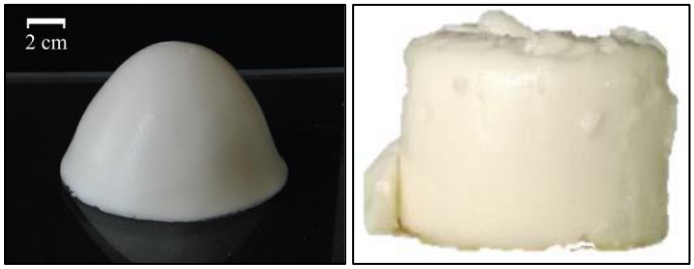

(c) (d)

Figure 2.6 Breast tissue-mimicking phantoms fabricated using oil-in-gelatin (Croteau et al., 2009; Di Meo et al., 2019; Mashal et al., 2011; Porter et al., 2011)

2.5.2 Oil-in-agar (Safflower Oil)

The phantom developed by Lazebnik et al. (2005) was then altered to offer improved flexibility and tissue-matching qualities by switching gelatin for the agar. Fabrication of a heterogeneous breast phantom, including skin, fat, fibro-glandular tissue, and tumor tissue was conducted (Ostadrahimi et al., 2009) (Figure 2.7 (a)). A 10 cm disc with a 4 cm thickness was created to hold samples of each tissue. The proposed phantom's relative permittivity closely resembles that of real breast tissue. Although there is a good contrast in conductivity, the conductivity is higher than that of real breast tissues. After that, regression models have been presented by Hahn and Noghanian (2012) as a systematic method for creating breast tissue phantoms that have the physiological and dielectric properties of real breast tissues (Figure 2.7 (b)). The regression model for this process was developed by examining various combinations and their dielectric properties.

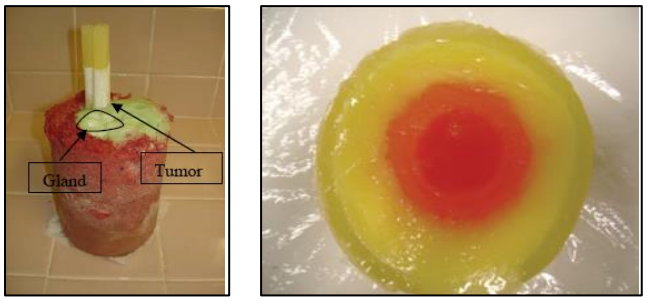

(a) (b)

Figure 2.7 Breast tissue-mimicking phantoms fabricated using oil-in-agar (Hahn & Noghanian, 2012; Ostadrahimi et al., 2009)

2.5.3 Oil-in-agar (Coconut oil and canola oil), Polyvinylpyrrolidone (PVP)

A breast tissue-mimicking phantom for combined microwave and ultrasound imaging is presented by Li et al. (2020). Agar was used as a base for all phantoms. It was found that polyvinylpyrrolidone (PVP) produces the most realistic results when mimicking tumor and fibroglandular tissues, whereas coconut oil and canola oil produced the most accurate results when mimicking skin and fat.

2.5.4 Oil-in-gelatin/ agar (Grapeseed Oil), Cornflour

In one experiment, a heterogeneous breast phantom was created using grapeseed oil (Abu Bakar et al., 2010, 2011) (Figure 2.8 (a)). Safflower oil was substituted for grapeseed oil (Lazebnik et al., 2005). For phantom glandular tissue, gelatin and grape seed oil was utilized, while agar was used in place of gelatin for phantom tumors. By combining milli-Q water and propylene glycol, fat tissue was created. Inserting several parts that stand in for tumors and glands gives it its heterogeneous structure. For at least 12 weeks following preparation, the generated breast phantom's dielectric constant fluctuation is stable, and it has a long lifespan. The measurements of the various components of the manufactured phantom have shown that the breast gland, tumor, and fat are reasonably mimicked. The created phantom is harmless, easy to handle, and has a lifelike shape. Then, Abu Bakar et al. (2011), created another heterogeneous breast